C. R. Physique 11 (2010) 472–479

Contents lists available at ScienceDirect

Comptes Rendus Physique

www.sciencedirect.com

Terahertz electronic and optoelectronic components and systems

Terahertz photomixers based on ultra-wideband horn antennas

Photomélangeurs térahertz à antennes cornet ultra-large bande

Alexandre Beck, Tahsin Akalin, Guillaume Ducournau, Emilien Peytavit, Jean-François Lampin *

Institut d'électronique de microélectronique et de nanotechnologie, UMR CNRS 8520, université des sciences et technologies de Lille, avenue Poincaré, B.P. 60069, 59652 Villeneuve d'Ascq, France

ARTICLE INFO

Article history:
Available online 8 July 2010

Keywords:
Terahertz waves
Horn antenna
Photomixing
Photodiode

Mots-clés :
Ondes térahertz
Antenne cornet
Photomélange
Photodiode

ABSTRACT

We review recent advances in the development of new terahertz photomixers based on the integration of an ultrafast photodetector with an ultra-wideband transverse electromagnetic wave horn antenna. We expose first a simplified theory of this antenna, the choice of the dimensions and the results of electromagnetic modeling. We expose then the technological process of the antenna and its integration with ultrafast photodetectors. In the last part we present a photomixing experiment and radiation patterns measurements.

RÉSUMÉ

Cet article expose le développement récent d'une nouvelle génération de photomélangeurs térahertz basés sur l'intégration d'un photodétecteur ultra-rapide avec une antenne ultra-large bande de type cornet à onde transverse électromagnétique. Nous exposons d'abord la théorie simplifiée de cette antenne puis le choix des dimensions et les résultats de simulations électromagnétiques. Nous exposons ensuite le procédé de réalisation technologique de l'antenne et son intégration avec des photodétecteurs ultra-rapides. Enfin nous présentons une expérience de photomélange et des résultats de mesures de diagrammes de rayonnement.

1. Introduction

1.1. Generation of CW terahertz radiation with photomixing

Powerful room-temperature solid-state terahertz sources are needed for promising applications such as spectroscopy, imagery, and telecommunications. Among them, widely tunable coherent continuous-wave (CW) sources with high spectral quality are ideal for spectroscopy. Optical frequency mixing (or photomixing) is a powerful technique for such applications since the optical beatnote can be tuned easily in the whole terahertz range. The first photomixing experiments were made two years after the demonstration of the first laser [1]. The mixing occurred in a biased bulk semiconductor placed in a microwave waveguide (1–10 GHz). During the following decades the mixing technique was used essentially to measure the

* Corresponding author.
E-mail address: jean-francois.lampin@isen.iemn.univ-lille1.fr (J.-F. Lampin).

1631-0705/$ – see front matter
doi:10.1016/j.crhy.2010.05.006

bandwidth of photodetectors, but not as a mm or sub-mm (or THz) source, because of the lack of robust large bandwidth photodetectors and of easily tunable powerful lasers.

With the advance of high-speed III–V photodetectors and solid-state lasers, interest in THz generation has been revived in the 1990s. The first photomixing experiments at THz frequencies were reported in 1995 in a low-temperature-grown GaAs (LTG-GaAs) photoconductor [2]. In this case, due to the high losses and the difficulty of fabrication of THz waveguides, the photoconductor was placed at the center of a wideband planar spiral antenna in order to radiate directly the THz signal in free-space. This configuration is also very interesting for spectroscopy applications. Since these initial experiments several variations of the photodetector and of the antenna were investigated in order to increase the generated power (for a review, see [3]). However, it seems difficult to increase the overall efficiency of photomixers: new photodetectors and new antennas are then needed. In this article we will concentrate essentially on a new antenna that allows new configurations.

1.2. Antennas for terahertz photomixers

If we focus on the antenna design for terahertz photomixers, we can cite the use of spiral [2], log-periodic [4] and bow-tie [5] as broadband antennas and dipole [5,6], slot [6], dual-dipole and dual-slot [7] as resonant antennas. All these antennas have planar metalizations patterned at the air/semiconductor interface and are simple to fabricate and to integrate with the photodetector. The photomixing source has a very wide tunability and for most applications the broadband antennas are ideal, we will focus on this type of antenna.

In order to obtain a bandwidth of one decade or more two principles are generally used for the design of an antenna: Rumsey's principle and the self-complementarity. An antenna verifies Rumsey's principle if its geometry can be defined only by angles [8]. It is commonly accepted as the first principle for the design of frequency independent antennas. In addition the self-complementarity is often used to smooth out the impedance variations. The radiation resistance of a self-complementary antenna in vacuum is $R = Z_0/2$ (Z_0 is the vacuum impedance) or 188.5 Ω. In the case of a photomixer half of the space is the semiconductor and the effective dielectric constant is: $R = Z_0/2\sqrt{\epsilon_{eff}}$ with $\epsilon_{eff} = (\epsilon_r + 1)/2$. For GaAs, $\epsilon_r = 13$, $\epsilon_{eff} = 7$, and $R = 71$ Ω. This impedance is much lower than the resistance of the LTG-GaAs photoconductor (typically 10 kΩ or more).

The fact that the antenna is patterned at the air/semiconductor interface has also another important consequence: most of the electromagnetic energy is radiated into the semiconductor because of its high permittivity. If a standard substrate is used (a few hundreds of μm thick), guided electromagnetic modes are excited and trapped into the wafer (surface waves) [9]. A standard solution is to attach a substrate lens of the same permittivity to the backside of the substrate [2,10,11]. This hemispherical or hyperhemispherical lens suppress the total internal reflection but high Fresnel reflection losses are still present. An anti-reflection coating can be deposited on the lens but it reduce considerably the bandwidth. The calculation of the radiation pattern of large bandwidth planar antennas coupled to a high permittivity substrate lens is a complicated electromagnetic problem and only a few articles give practical measurements [12,13]. Estimations are difficult, but it seems that the overall efficiency of this standard approach is limited. Another drawback is related to the practical aspect: placing with precision this lens and bonding it without introducing parasitic reflections is critical and add some costs.

2. The terahertz TEM horn antenna

2.1. Definition the TEM horn

We can define the characteristics of an ideal antenna for THz photomixers: very large bandwidth (at least 10:1), high radiation resistance, constant radiation pattern and impedance over frequency. In addition, the antenna must be monolithically integrable with the photodetector. Another desirable feature is that the antenna does not radiate into the semiconductor substrate. Then a high permittivity substrate-lens is not needed: the need of precise alignment, the losses and cost of this lens are avoided.

A simple example of Rumsey's principle is the infinite bow-tie antenna. In this case two conducting triangular plates are in the same plane and the angle of each plate at the drive point is defined by 2α. However, Rumsey's principle is also fulfilled if the triangles are in two different planes forming an angle 2β (Fig. 1a). This geometry is called the infinite TEM horn antenna (TEMHA). This name comes from the geometrical similarity with the well-known pyramidal horn, but here, two lateral conducting walls are not present and a TEM spherical wave is allowed inside the antenna. One of the first description of this antenna was made by L. Brillouin [14]. Its characteristic impedance can be calculated analytically or numerically [15].

This TEMHA is interesting because it is frequency independent and it gives more degrees of freedom in the design than the bow-tie antenna. However, unfortunately, it is also a non-planar structure which is difficult to fabricate at THz frequencies with a standard microelectronics process. A modified version of the TEMHA is more easy to fabricate: the monopole TEMHA (Fig. 1b). In this case the lower triangle is replaced by an infinite conductive plane placed in the symmetry plane of the antenna perpendicular to the electric field. This configuration is more simple (only one triangle) and is particularly adapted for a monolithic integration on a semiconductor substrate because the radiation is confined in a half space. If a metal ground plane is deposited on the substrate and a triangle is formed above it, in principle, no radiation should occur

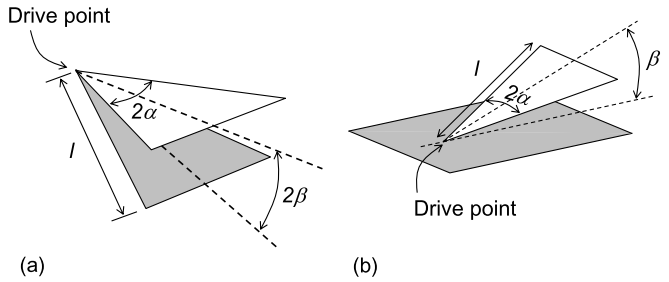

Fig. 1. Geometry of the TEMHA (a). Geometry of the monopole configuration of the TEMHA (b).

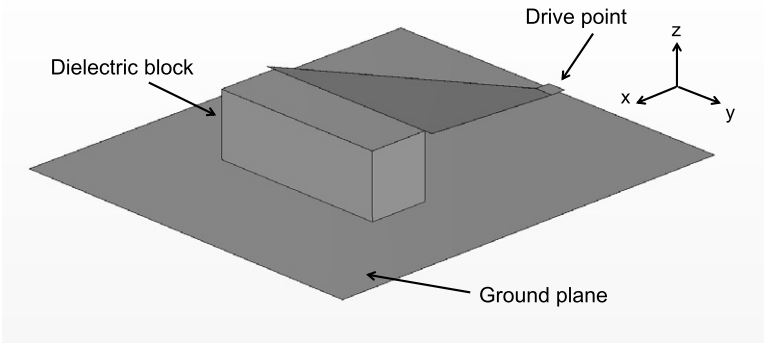

Fig. 2. View of the simulated TEMHA.

into the semiconductor and no substrate lens is needed. In this configuration the TEMHA forms a tapered microstripline whose characteristic impedance is fixed by the W/h ratio (W is the width of the strip, h the height of the strip) and naturally by α and β.

2.2. Definition of the dimensions

To design a practical monopole THz-TEMHA we must define α, β and l the length of the triangle. In our study, β was fixed around 10–15° in order to optimize the radiation pattern [16] and by taking into consideration the technological and mechanical aspects. α is then fixed by taking into account the targeted impedance, the radiation pattern and also some mechanical considerations. $\alpha = 23.4°$ was chosen in order to obtain an impedance of 50–70 Ω compatible with standard transmission lines. This impedance is also close to the impedance of planar wideband antennas and a comparison is then possible. The practical TEMHA is not infinite. In fact the length l of the triangle defines the low frequency cut-off of the antenna f_l [16]. For the chosen angles, the impedance cut-off is obtained for $l/\lambda \simeq 1$. We have chosen $f_l = 100$ GHz ($l = 3$ mm) in order to preserve the wide bandwidth of the photomixer and also to limit the size of the antenna. Taking into account α we can calculate the length of the base of the triangle which is 2.6 mm. In order to obtain the targeted impedance the base of the triangle must be lifted between 500 and 800 μm above the ground plane. Maintaining the correct value of the angle can be achieved by placing a small dielectric block near the base of the triangle. The ground plane is also finite, in general it will be taken larger than the triangle.

2.3. Electromagnetic modeling

We have performed 3D electromagnetic simulations of the described TEMHA with Microwave Studio (CST). Fig. 2 shows a view of the simulated structure. The dimensions of the triangle were given in the previous paragraph. A low permittivity dielectric block ($\epsilon = 2.1$) is placed in front of the TEMHA, its dimensions are $2400 \times 800 \times 850$ μm^3. The dimensions of the ground plane are 5.5×5 mm^2. All the metallizations are modeled with perfect conductors and the losses of dielectrics are also assumed to be negligible.

The calculated S_{11} parameter (reflection coefficient) is lower than -10 dB from 100 GHz to more than 1 THz, it confirms the ultra-large bandwidth of this antenna (more than one decade). The calculated radiation patterns are plotted on Fig. 3 for typical frequency values and show the behavior of the main lobe.

At 200 GHz, 500 GHz and 700 GHz, the angle between the main lobe and the ground plane (xy-plane) is 32°, 13° and 10°, respectively. The values at other frequencies and the isotropic directivity are given in Table 1. In the low frequency part ($\simeq 100$ GHz, $l/\lambda \simeq 1$), the antenna has a relatively low directivity and the direction of the main lobe tends to be high even if it is far from being perpendicular to the ground plane. When the frequency increases the main lobe becomes narrower

Fig. 3. 3D radiation patterns of the TEMHA. The directivity scale is linear and is the same for all the patterns.

Table 1
Value and direction of the maximum isotropic directivity in the *xz*-plane versus frequency. The angles are given with respect to the ground plane.

Frequency (GHz)	Direction (°)	Directivity (dBi)
200	32	13.4
250	25	14.2
500	13	15.9
700	10	17.4
800	8	16.6
1000	7	13.8

in the horizontal and vertical planes and the directivity increases. The direction of the main lobe becomes also closer to the ground plane. Above 800 GHz ($l/\lambda > 8$) the main lobe slowly splits in two in the *xy*-plane. This effect decreases the directivity of the antenna at high frequency. Between these two regions, in the 100–800 GHz range, there is a wide frequency band where the antenna has a good directivity and a single main lobe which is interesting for applications. The ground plane size modifies slightly the radiations patterns but the general tendency remains the same. The radiated beam is linearly polarized orthogonally to the ground plane.

The magnitude of the electric field inside and near the TEMHA for different frequencies is plotted in Fig. 4. The gray scale is chosen in order to show clearly the phase fronts. We can observe clearly that a spherical wave propagates inside the horn. Near the right part of the triangle, at low frequency (250 GHz) the phase difference between the principal axis of the antenna and the both sides is negligible but at higher frequencies (above 700 GHz) it is not the case. The effect of this phase non-uniformity can be seen in front of the dielectric block. This phase difference is the origin of the main lobe splitting at the highest frequency region. Naturally, a scaling of the antenna is possible to cover other frequency ranges: for example, a 1.5 mm long triangle will have a low frequency cut-off at $f_l = 200$ GHz and a high frequency splitting of the main lobe near 1600 GHz due its to shorter length and lower dephasing.

3. Technological aspects

3.1. TEMHA process

The main issue consists in the integration of the TEMHA, which is inherently 3D, to a transmission line, a coplanar waveguide (CPW), connected to the photodetector. The process flow is shown in Fig. 5.

First, the ground plane and the CPW are patterned by means of standard photolithography, electron-beam evaporation and lift-off technique on the insulating substrate. Then a deep-UV photoresist layer is deposited and exposed to define the future drive point of the antenna. This resist will be used as a sacrificial layer. A 4-μm-thick gold film is then deposited and the triangle is patterned thanks to chemical etching. Finally, the structures are released by etching the sacrificial layer and dried in a supercritical CO_2 dryer. The thickness of the gold film has been determined empirically: on the one hand, curvature induced by residual stress in the film is inversely proportional to its thickness, but on the other hand, despite of the supercritical CO_2 drying, a minimal amount of curvature is necessary to avoid sticking to the ground plane. A radius of curvature of about 15 mm is achieved for the triangle fabricated with this process. After releasing, the triangle is lifted by means of a micromanipulator up to the desired height and brazed to a copper-cladded polytetrafluoroethylene (PTFE) block (height = 800 μm). The photodetector is biased thanks to a 20-μm-diameter gold wire also brazed on the block.

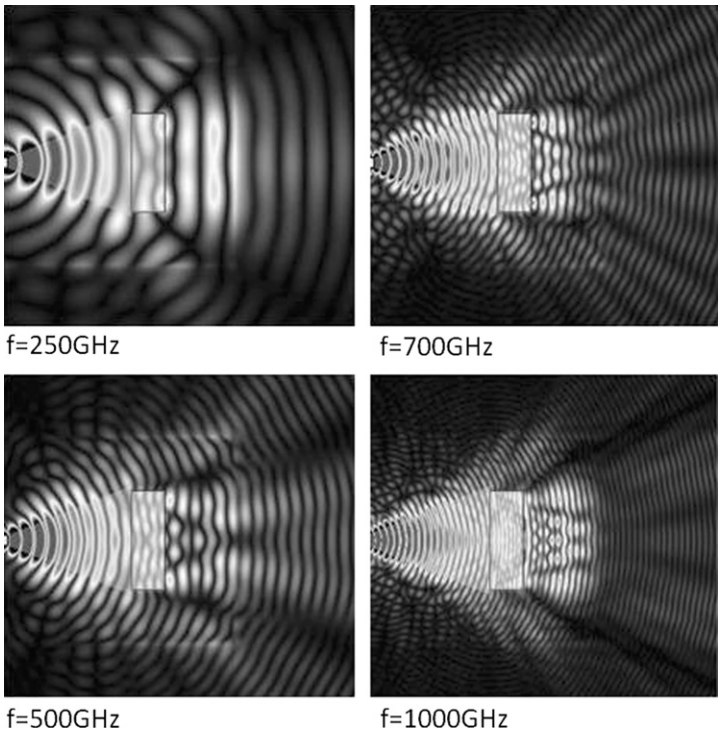

Fig. 4. Magnitude of the electric field in a plane just above the ground plane at various frequencies.

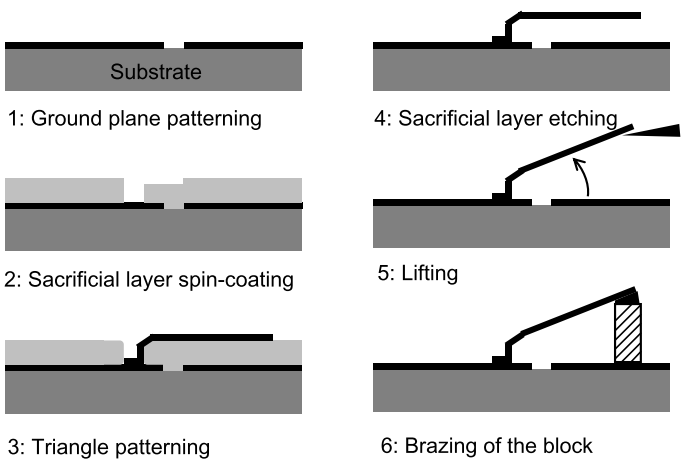

Fig. 5. Process flow of the TEMHA (side view, not to scale).

3.2. Integration with ultrafast photodetectors

To realize a photomixer the antenna must be coupled with an ultrafast photodetector. Two types of photodetectors have been integrated with the TEMHA: LTG-GaAs photoconductors sensitive at 0.78 µm [17–19] and InGaAs/InP uni-traveling-carrier photodiodes sensitive at 1.55 µm (UTC-PD) [20]. Details about the photodetectors and their monolithic integration with the TEMHA are given in the articles. A typical image of the final device is shown in Fig. 6. The PTFE block, the bonding and also the slight curvature of the triangular metalization are visible. In the following part of the article we will show results obtained with a TEMHA integrated with an InGaAs/InP UTC-PD.

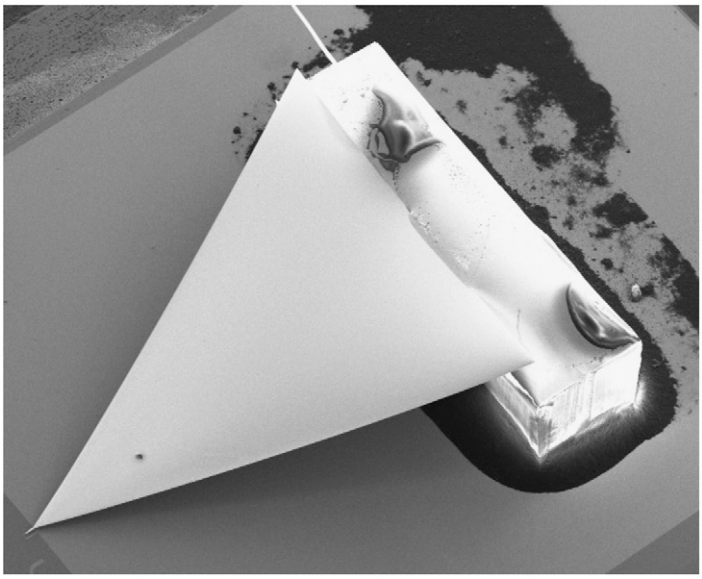

Fig. 6. Scanning electron microscope picture of a TEMHA integrated with a UTC-PD.

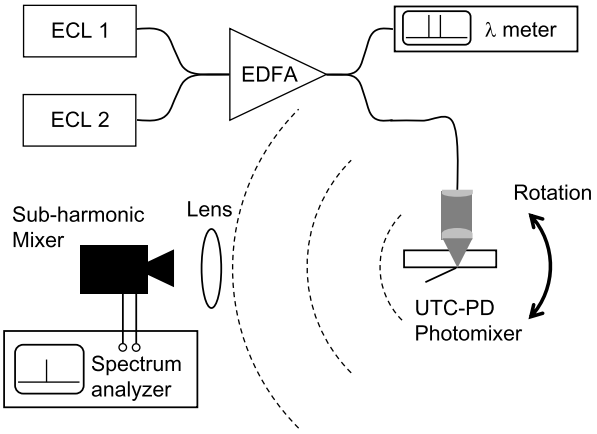

Fig. 7. Experimental setup.

4. Photomixing experiments

4.1. Experimental setup

The experimental set-up is shown in Fig. 7. Two 1.55 μm external cavity lasers are coupled into a single monomode optical fiber. These two wavelengths are simultaneously amplified with an erbium-doped fiber amplifier. 10% of the output is used to monitor the two optical lines thanks to a wavelength meter. 90% of the optical signal is focused on the backside of the photomixer thanks to the fiber-coupled collimator and an aspheric lens.

The millimeter or sub-millimeter beam is radiated by the TEMHA photomixer and collected by a 25 mm diameter polymethylpentene (TPX) lens placed at 20 cm of the photomixer. It focuses the wave in a conical horn connected to a WR2.8 (260–400 GHz) or a WR1.9 (400–600 GHz) Schottky diode sub-harmonic mixer connected to a spectrum analyzer. Only a part of the radiated beam is collected by the lens but a signal to noise ratio of about 30–40 dB is obtained for a UTC-PD photocurrent of 300–400 μA and a resolution bandwidth of 100 kHz. This signal dynamic range is sufficient for radiation pattern measurements including side lobes.

The photomixer is placed on a computer controlled motorized rotation stage which allows a 360° rotation thanks to the flexibility of the optical fiber. It was checked that the drive point of the triangle of the TEMHA was positioned very close to the rotation axis. With this configuration, a rotation in a plane orthogonal to the ground plane (*xz*-plane or E-plane) is obtained.

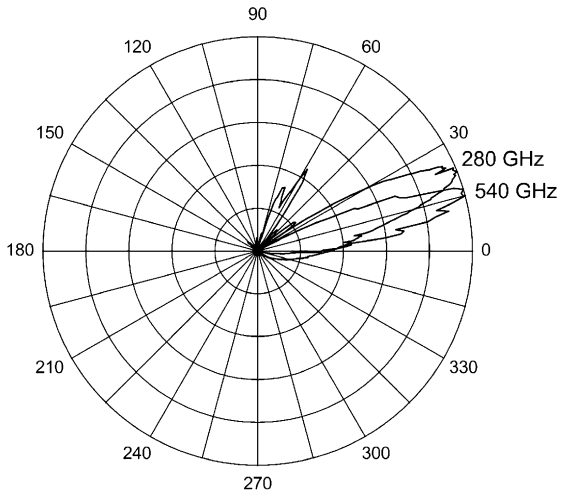

Fig. 8. Normalized E-plane radiation patterns of the TEMHA at 280 and 540 GHz (linear scale, 0° is the direction of the ground plane).

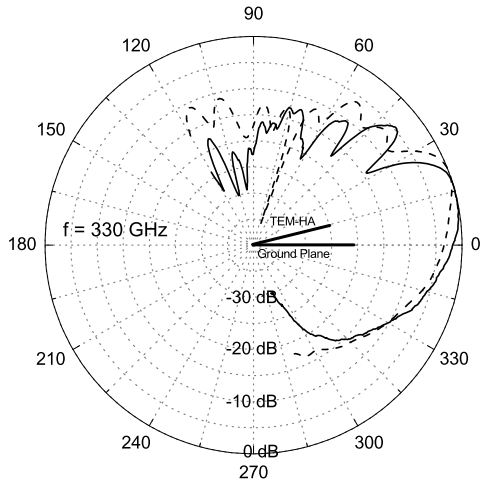

Fig. 9. Normalized E-plane radiation patterns of the TEMHA at 330 GHz (solid line: measurement, dashed line: simulated data).

4.2. Measurements of radiation patterns

Fig. 8 shows the radiation patterns measured at 280 and 540 GHz. The main lobe is tilted with respect to the ground plane: 22° and 16° respectively. The 3 dB beamwidth is about 18–20°. These angles are close to the expected values. Some side lobes are also measured in the 30–120° range.

A more detailed comparison is possible in Fig. 9 at 330 GHz. Side lobes are more visible thanks to a logarithmic scale. The simulated and measured main lobes are close but for the side lobes the differences are more pronounced. These differences can be attributed to the curvature of the triangle and to the gold wire which are taken into account in the simulations.

5. Conclusion

The TEMHA is a high-directivity ultra-wideband antenna suitable for applications like wireless transmissions, imagery and spectroscopy. A monolithic technological process has been developed to realize TEMHA at THz frequencies. In this range, it is very compact and does not need a silicon lens like planar spiral or log-periodic antennas. Another important consequence is that the substrate can be chosen with more freedom because there is no THz propagation through it. As an example we can mention that a vertically integrated photomixer based on a LTG-GaAs layer bonded on a low-cost conductive silicon wafer was developed recently [19].

Acknowledgements

This work was supported by the Région Nord Pas de Calais and the DGA (contract 06.34.021).

References

[1] M. DiDomenico, R.H. Pantell, O. Svelto, J.N. Weaver, Optical frequency mixing in bulk semiconductors, Appl. Phys. Lett. 1 (1962) 77.
[2] E.R. Brown, K.A. McIntosh, K.B. Nichols, C.L. Dennis, Photomixing up to 3.8 THz in low-temperature-grown GaAs, Appl. Phys. Lett. 66 (1995) 285.
[3] S. Matsuura, H. Ito, K. Sakai (Eds.), Terahertz Optoelectronics, Topics Appl. Phys., vol. 97, Springer, 2005, p. 157.
[4] R. Mendis, C. Sydlo, J. Sigmund, M. Feiginov, P. Meissner, H.L. Hartnagel, Spectral characterization of broadband THz antennas by photoconductive mixing: toward optimal antenna design, IEEE Antennas Wireless Propag. Lett. 4 (2005) 85.
[5] S. Matsuura, M. Tani, K. Sakai, Generation of coherent terahertz radiation by photomixing in dipole photoconductive antennas, Appl. Phys. Lett. 70 (1997) 559.
[6] S. Verghese, K.A. McIntosh, E.R. Brown, Highly tunable fiber-coupled photomixers with coherent terahertz output power, IEEE Trans. Microwave Theory Tech. 45 (1997) 1301.
[7] S. Duffy, S. Verghese, K. McIntosh, A. Jackson, A. Gossard, S. Matsuura, Accurate modeling of dual dipole and slot elements used with photomixers for coherent terahertz output power, IEEE Trans. Microwave Theory Tech. 49 (2001) 1032.
[8] V.H. Rumsey, Frequency Independent Antennas, Academic Press, New York, 1966.
[9] D.B. Rutledge, D.P. Neikirk, D.P. Kasilingam, K.J. Button (Eds.), Infrared and Millimeter Waves, vol. 10, Academic Press, New York, 1983, p. 1.
[10] D.P. Neikirk, D.B. Rutledge, M.S. Muha, Far-infrared imaging antenna arrays, Appl. Phys. Lett. 40 (1982) 203.
[11] C. Fattinger, D. Grischkowsky, Terahertz beams, Appl. Phys. Lett. 54 (1989) 490.
[12] P. Uhd Jepsen, S.R. Keiding, Radiation patterns from lens-coupled terahertz antennas, Opt. Lett. 20 (1995) 607.
[13] J.L. Hesler, L. Liu, H. Xu, Y. Duan, R.M. Weikle, The development of quasi-optical THz detectors, in: Joint 33rd International Conference on Infrared and Millimeter Waves and 16th International Conference on Terahertz Electronics, Pasadena, 2008.
[14] L.N. Brillouin, Broad band antenna, U.S. Patent 2,454,766, November 30, 1948.
[15] R.T. Lee, G.S. Smith, On the characteristic impedance of the TEM horn antenna, IEEE Trans. Antennas Propag. 52 (2004) 315.
[16] R.T. Lee, G.S. Smith, A design study for the basic TEM horn antenna, IEEE Antennas Propag. Mag. 46 (2004) 86.
[17] E. Peytavit, J.-F. Lampin, T. Akalin, L. Desplanque, Integrated terahertz TEM horn antenna, Electron. Lett. 43 (2007) 73.
[18] E. Peytavit, A. Beck, T. Akalin, J.-F. Lampin, F. Hindle, C. Yang, G. Mouret, Continuous terahertz-wave generation using a monolithically integrated horn antenna, Appl. Phys. Lett. 93 (2008) 111108.
[19] E. Peytavit, J.-F. Lampin, F. Hindle, C. Yang, G. Mouret, Wide-band continuous-wave terahertz source with a vertically integrated photomixer, Appl. Phys. Lett. 95 (2009) 161102.
[20] A. Beck, G. Ducournau, M. Zaknoune, E. Peytavit, T. Akalin, J.-F. Lampin, F. Mollot, F. Hindle, C. Yang, G. Mouret, High efficiency uni-travelling-carrier photomixer at 1.55 μm and spectroscopy application up to 1.4 THz, Electron. Lett. 44 (2008) 1320.